Investigation into Return Loss Characteristic of Graphene Oxide/Zinc Ferrite/epoxy composite at X-band frequency

Yi Lin Chan[1], Kok Yeow You[2], Mohd Zul Hilmi Mayzan[1], Mohamad Ashry Jusoh[3], Zulkifly Abbas[4], and Fahmiruddin Esa[1,*]

[1] *Material Physics Laboratory, Department of Physics and Chemistry, Faculty of Applied Sciences and Technology, Universiti Tun Hussein Onn Malaysia, 84600 Pagoh, Muar, Johor, Malaysia*
[2] *Radar Laboratory, School of Electrical Engineering, Faculty of Engineering, Universiti Teknologi Malaysia, 81310 Skudai, Johor Bahru, Johor, Malaysia*
[3] *Faculty of Industrial Sciences and Technology, Universiti Malaysia Pahang, Lebuhraya Tun Razak, 26300 Gambang, Kuantan, Pahang, Malaysia*
[4] *RF Microwave Laboratory, Department of Physics, Faculty of Science, Universiti Putra Malaysia, Serdang, 43400 Seri Kembangan, Selangor, Malaysia*
[*] *Corresponding author. E-mail: fahmir@uthm.edu.my*

Received: May. 09, 2019; Accepted: Nov. 05, 2019

Composite absorbing material is a branch of study that relates electromagnetic compatibility to radio and microwave frequency applications. Thus, many researchers have been made to focus on the composite fabrication and its characteristic of microwave signal performance. Generally, a light weight, high absorption and low cost absorber is highly demanded. Therefore, this work aims to investigate the return loss (RL) characteristics of graphene oxide/zinc ferrite/epoxy composite in the range of frequency 8.2 GHz to 12.4 GHz. The structural patterns of graphene oxide (GO) and Zn ferrite ($ZnFe_2O_4$) were confirmed by X-ray diffraction (XRD). Surface morphologies of the composites were characterized by Coxem Table Top SEM equipped with an energy dispersive spectroscopy (EDS) system and the tracing elements were identified. The bulk density of $ZnFe_2O_4$ could be reduced by addition of GO based on the measurement results. Electromagnetic properties were calculated using Nicolson-Ross-Weir (NRW) conversion technique based on measured S-parameters by vector network analyzer (VNA). Complex relative permittivity increases as the GO content increases due to the increment of dipolar polarization whereas a minor change occurred in permeability. Generally, the dissipation factor happens in the range of 10 – 11 GHz for both properties. A minimum RL is found to be -12.7 dB at 10.5 GHz with 2.35 mm for 3-GO-$ZnFe_2O_4$ composite sample. The RL performance of the sample could be tuned as low as -55 dB using higher thickness samples.

Keywords: Graphene oxide; Zinc ferrite; Composite materials; Return loss; Electromagnetic properties

http://dx.doi.org/10.6180/jase.202012_23(4).0003

1. Introduction

Recently, electromagnetic (EM) pollution has emerged due to the rapid growth of electronic devices in telecommunication area such as wireless communication industry and military [1]. The development of microwave electronic devices without EM control will affect human health and degrade the devices performance [2]. Thus, microwave absorbing materials have been developed in order to reduce the pollution from the telecommunication devices [3]. Nevertheless, the most practical materials with low density, light weight, low cost, high absorption power, wideband absorption capability and design flexibility are being progressively investigated [4].

Microwave absorbing materials consist of matrix and filler. Polymer is usually used as the matrix for its design flexibility and low processing temperature [5]. Epoxy is one

of the best polymer candidates because it is commercially available, resistant to corrosion and easily processed [6]. A good microwave absorbing material should possess low reflection and high absorption properties [7] that depend on relative permeability and permittivity, impedance matching and microstructure of the material [8]. Introduction of dielectric and magnetic fillers into the polymer matrix could enhance microwave absorption properties [4, 9–11]. This distinct property makes graphene and graphene-based composites appear as promising candidates in microwave absorption field [12, 13].

Zinc ferrites ($ZnFe_2O_4$) have been studied extensively in microwave absorbing material due to its microwave absorption properties [14], unique electrical [15] and magnetic properties [16]. Many methods have been developed to fabricate $ZnFe_2O_4$ such as co-precipitation [17], electrodeposition [18], ball milling [19, 20] and sol-gel [21]. However, $ZnFe_2O_4$ has a high density that restricts its use in light weight application. One of the effective ways to overcome the high density of $ZnFe_2O_4$ is the addition of a dielectric filler into the microwave absorbing composite material [22]. Therefore, graphene oxide (GO) is introduced due to its low density, large specific surface area, residual effect and high dielectric loss [23–26].

Composite materials with dielectric and magnetic fillers have appeared as a promising microwave absorbing material due to its excellent dielectric and magnetic properties along with lesser density and resistance to chemical [27, 28]. Many preparation methods have been developed to prepare the composite materials such as solvothermal method [29], physical mixing [30], chemical synthesis [31], chemical vapour deposition [32] and arc discharge [33].

In this paper, we fabricated epoxy composites by dispersing GO and $ZnFe_2O_4$ as dielectric and magnetic filler, respectively into an epoxy matrix. Structures for both fillers were confirmed by XRD. The epoxy composite samples were analyzed by Coxem Table-Top SEM equipped with an EDS system. EM properties were calculated using NRW conversion technique based on S-parameters via two-port rectangular waveguide reflection/transmission measurement. RL characteristic of composites at different thicknesses was then investigated via transmission line equation.

2. Theory and formula

2.1. NRW Conversion Technique

Raw data of complex scattering reflection coefficient, S_{11} and scattering transmission coefficient, S_{21} of the finite thickness sample filled in rectangular waveguide holder were measured by VNA. The actual value of reflection coefficient, Γ and transmission coefficient, T can be deduced from the measured raw data of complex S_{11} and S_{21} as [34]:

$$\Gamma = \frac{S_{11}^2 - S_{21}^2 + 1}{2S_{11}} \pm \sqrt{\left(\frac{S_{11}^2 - S_{21}^2 + 1}{2S_{11}}\right)^2 - 1} \quad (1)$$

$$T = \frac{S_{11}^2 + S_{21}^2 + \Gamma}{1 - (S_{11}^2 + S_{21}^2)\Gamma} \quad (2)$$

The complex relative permittivity $\varepsilon_r (= \varepsilon_r' - j\varepsilon_r'')$ and permeability $\mu_r (= \mu_r' - j\mu_r'')$ of sample can be calculated by NRW conversion technique.

$$\varepsilon_r = \frac{\lambda_0^2}{\mu_r}\left[\frac{1}{\lambda_c^2} - \left[\frac{1}{2\pi L} ln\left(\frac{1}{T}\right)\right]^2\right] \quad (3)$$

$$\mu_r = \frac{1+\Gamma}{\Lambda(1-\Gamma)\sqrt{\frac{1}{\lambda_0^2} - \frac{1}{\lambda_c^2}}} \quad (4)$$

$$\frac{1}{\Lambda^2} = -\left(\frac{1}{2\pi L} ln\left(\frac{1}{T}\right)\right)^2 \quad (5)$$

where λ_0 = free space wavelength, λ_c = cut-off wavelength, L = sample thickness.

2.2. Return Loss

RL characteristic of composite materials can be calculated using transmission line theory [35]:

$$RL(dB) = 20lg\left|\frac{Z_{in} - 1}{Z_{in} + 1}\right| \quad (6)$$

$$Z_{in} = \sqrt{\frac{\mu_r}{\varepsilon_r}} tanh\left(j\frac{2\pi f d}{c}\sqrt{\mu_r \varepsilon_r}\right) \quad (7)$$

where Z_{in} = input impedance of the absorber (epoxy composite material), ε_r and μ_r are complex relative permittivity and permeability of absorber, f = frequency of the incident electromagnetic wave, d = sample thickness and c = velocity of light in the free space.

3. Experimental setup

3.1. Materials

ZnO (99% purity), Fe_2O_3 (99% purity) and GO nano powder (99% purity, 6 – 8 nm) were obtained from Alfa Aesar, Sigma-Aldrich and Sky Spring Nanomaterials, Inc., respectively.

3.2. Preparation of $ZnFe_2O_4$

$ZnFe_2O_4$ powder was prepared by solid state reaction method. Raw materials of ZnO and Fe2O3 were weighted using high precision (±0.0001) digital analytical balance (Mettler Toledo XS64). The raw materials were mixed and ground using agate mortar for 2 hours. The well-mixed powders were put in alumina crucible and then sintered

Table 1. Composition of composite materials.

Sample	Epoxy matrix		$ZnFe_2O_4$		GO	
	g	wt. %	g	wt. %	g	wt. %
$ZnFe_2O_4$	3.00	60	2.00	40	0.00	0
GO	4.85	97	0.00	0	0.15	3
1-GO-$ZnFe_2O_4$	3.00	60	1.95	39	0.05	1
3-GO-$ZnFe_2O_4$	3.00	60	1.85	37	0.15	3

Table 2. Thickness of composite materials after grinding.

Sample	Thickness (mm)
$ZnFe_2O_4$	2.46
GO	2.28
1-GO-$ZnFe_2O_4$	2.21
3-GO-$ZnFe_2O_4$	2.35

using Protherm box furnace for 5 hours at 1000°C with heating and cooling rate of 5°C/min. After heating, the sintered $ZnFe_2O_4$ powder was ground for an hour using agate mortar to ensure particles' homogeneity. Next, the ground $ZnFe_2O_4$ powder was sintered again at the same temperature and heating/cooling rate as earlier. The double sintered $ZnFe_2O_4$ powder was ground and sieved into 50 μm.

3.3. Preparation of Epoxy Composite Filled with $ZnFe_2O_4$ and GO

Table 1 shows the preparation of 5 g of ZnFe2O4, GO and epoxy composite GO-$ZnFe_2O_4$, which is based on different weight percents (1 wt. % and 3 wt. %) of GO. The weighed powders were mixed and ground thoroughly using agate mortar for 15 minutes. The epoxy resin and hardener were prepared in 2:1 ratio and mixed. Epoxy resin was chosen among the other polymer matrixes in this study because of its resistance to corrosion and ease of processing. The well-mixed powders were dispersed in the epoxy matrix and stirred gently to ensure uniform distribution with a minimum of bubble formation. The mixture was poured into rectangular sample holder with dimension of 22.86 x 10.16 mm and left to solidify under room temperature for 24 hours. Then, the solid epoxy composites were ground to ensure a flat surface was obtained. Fig. 1 shows epoxy composites GO-$ZnFe_2O_4$ with various wt. % of GO and $ZnFe_2O_4$ before and after grinding. Table 2 shows the thickness of each sample after grinding process.

3.4. Measurement Method

The structural patterns of $ZnFe_2O_4$ and GO powders were determined using XRD (Rigaku MiniFlex II Cu K_α radiation (λ= 1.5418 Å, 30 kV, 15 mA) over an angular range of 20° to 70° of 2θ in continuous scan mode with a step width of 0.02°. The densities of epoxy composites GO-$ZnFe_2O_4$ were measured using Mettler Toledo XS64 model density kit that is based on Archimedes principle (Fig. 2(a)). The morphologies of epoxy composites GO-$ZnFe_2O_4$ were characterized using Coxem Table-Top SEM equipped with an EDS system. The S-parameters of reflection S_{11} and transmission S_{21} coefficients were measured using Keysight E5071C VNA in the range of 8.2 – 12.4 GHz X-band frequency region. A rectangular sample holder was adjoined an X-band coax-waveguide adapter as shown in Fig. 2(b) while Fig. 2(c) shows the VNA set up for S-parameters measurement.

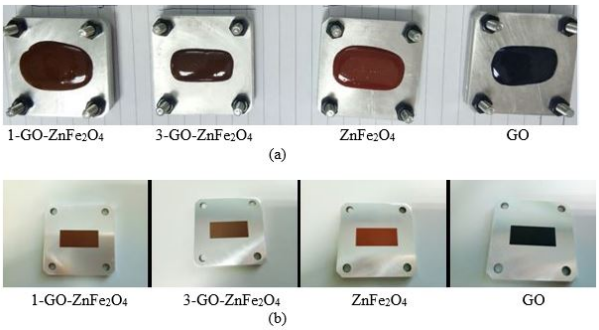

Fig. 1. Cured epoxy composite materials with various wt. % of GO and $ZnFe_2O_4$ (a) before and (b) after grinding.

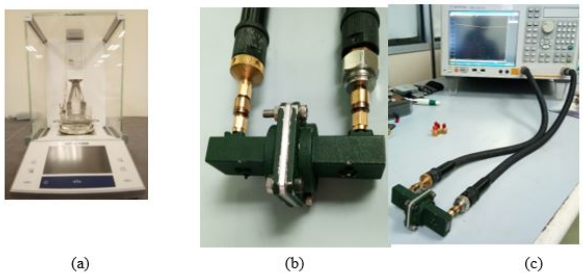

Fig. 2. Flow chart of the FVS-KELM method in the training phase.

4. Result discussions

Fig. 3 shows XRD pattern of $ZnFe_2O_4$ and GO powder. It can be observed that the diffraction peaks at 29.92°, 35.27°, 36.87o, 42.85°, 53.11°, 56.63° and 62.21° could be indexed to (220), (311), (222), (400), (422), (511) and (440) the face centered cubic (FCC) $ZnFe_2O_4$ phase (JCPDS 00-022-1012) [36–38], indicating that a formation of well crystallized $ZnFe_2O_4$ via solid state method. Meanwhile, the diffraction peaks of GO powder can be indexed to graphite phase (JCPDS 00-041-1487) [39–41]. This is due to the compression of tiny GO powder in the sample holder hence it looks

Table 3. Bulk density of composite materials.

Reading	$ZnFe_2O_4$	GO	1-GO-$ZnFe_2O_4$	3-GO-$ZnFe_2O_4$
1^{st}	1.641	1.138	1.647	1.626
2^{nd}	1.645	1.140	1.651	1.627
3^{rd}	1.640	1.139	1.651	1.622
4^{th}	1.645	1.135	1.654	1.624
5^{th}	1.643	1.136	1.642	1.623
Average	1.643	1.138	1.649	1.624

like a solid. Noticeably, a sharp peak at 2θ = 26.4° (002) can be observed implying that the hexagonal structured carbon atoms present in graphite [40, 42]. A broader peak of graphite plane (002) can be seen at 56.5°, which is associated with the partial crystalline behavior and lattice distortion of graphite structure [40, 43]. Density measurement shows that the addition of GO filler from 1 wt. % to 3 wt. % decreases the density of epoxy composites GO-$ZnFe_2O_4$ as could be seen in Table 3. GO possesses large surface area which results in increment and reduction of volume and density, respectively for each epoxy composite GO-$ZnFe_2O_4$ [23, 44–46].

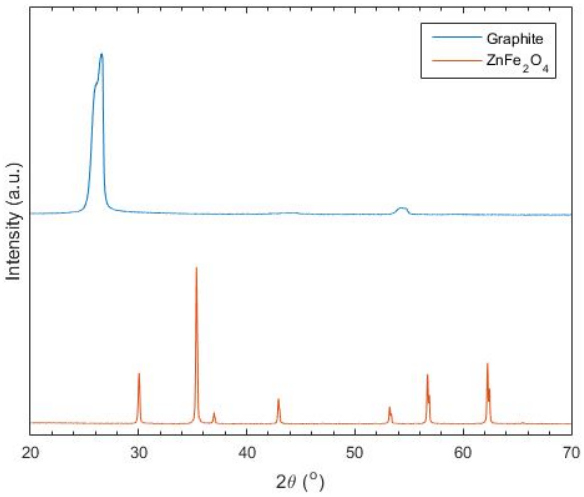

Fig. 3. XRD patterns of $ZnFe_2O_4$ and GO

Fig. 4 demonstrates SEM images of epoxy containing GO and 3-GO-$ZnFe_2O_4$. The respective EDS results are shown accordingly with point scanned in yellow circles. Random and uniform dispersion of GO and 3-GO-$ZnFe_2O_4$ particles are found in the epoxy matrix. This is due to the continuous stirring process during the composite sample preparation. The presence of Au element in the respective EDS tracing is due to the coated layer on the surface of composites. All the constituent elements C, O, Zn, Fe are present in the epoxy composite 3-GO-$ZnFe_2O_4$, as shown in Fig. 4(b), indicating that it is successfully developed.

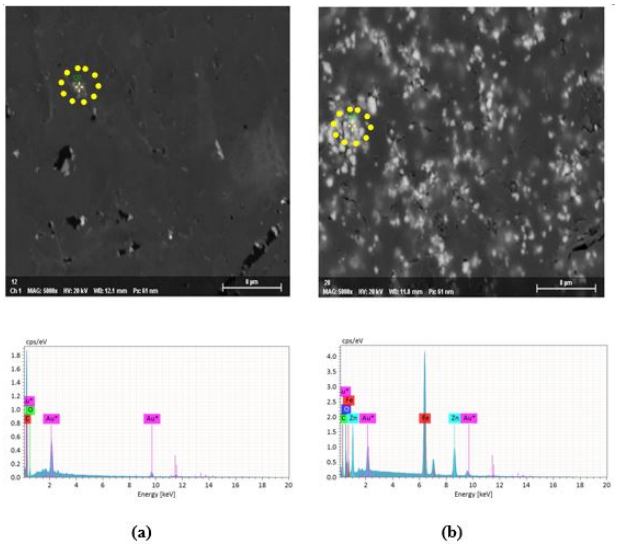

Fig. 4. Morphology and EDS element tracing of (a) GO and (b) 3-GO-$ZnFe_2O_4$.

Fig. 5 demonstrates the result of S-parameter measurement, S_{11} and S_{21} using rectangular waveguide at X-band frequency. The scattering reflection coefficient, S_{11} for epoxy containing GO is significantly higher than $ZnFe_2O_4$, indicating a strong electronic conductivity, σ that could be related to the dielectric loss factor, ε'' [38, 47, 48].

$$\sigma = \omega \varepsilon_0 \varepsilon' \tag{8}$$

The 1 wt. % and 3 wt. % addition of GO together with $ZnFe_2O_4$ inside the epoxy display a respectable increment in S_{11} while maintaining 40% of total fillers. Besides, the 3-GO-$ZnFe_2O_4$ in the epoxy is less densely packed than the 1-GO-$ZnFe_2O_4$ since the GO has lower particle density [47, 49, 50]. However, the scattering transmission coefficient, S_{21} is inversely proportional to the S_{11} due to the decrement in amount of incident electromagnetic wave penetrate through the sample and also due to the signal loss enhancement. Generally, the loss mechanism for all samples is prominently caused by material absorption along the frequency range since all the measurements were conducted using the closed system technique. Thus, the loss percentage in the material could be assessed using Equation 9 as shown in Fig. 6 where the dimensionless material absorption (A) multiplied by 100, such value signifies percentage of material absorption of composite material.

$$A = 1 - |S_{11}|^2 - |S_{21}|^2 \tag{9}$$

It can be observed that the overall absorption ratio per-

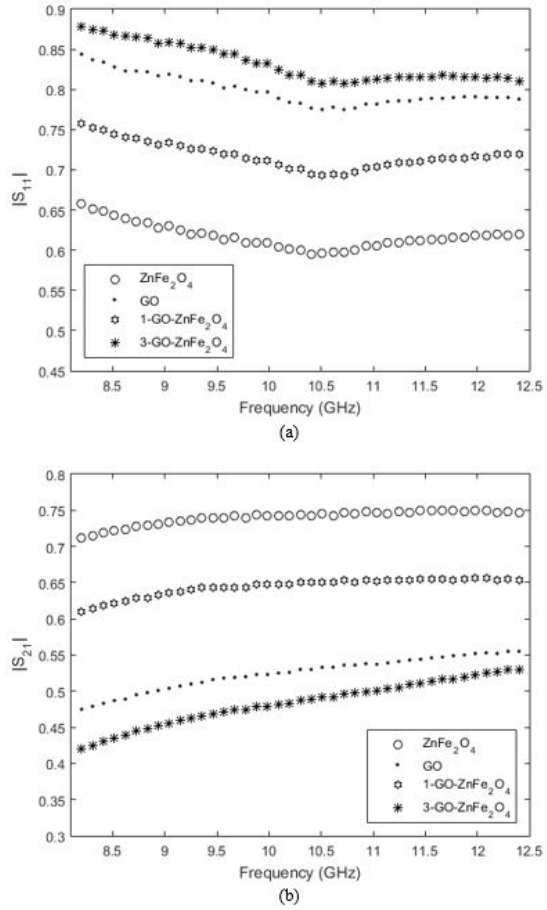

Fig. 5. Measured S-parameters of (a) and (b) .

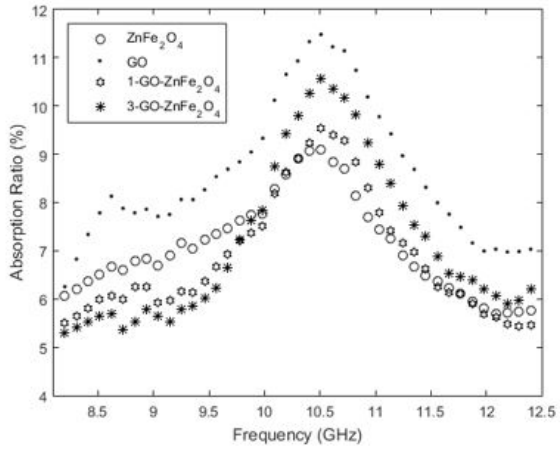

Fig. 6. Absorption ratio of epoxy composites GO-ZnFe2O4.

centage has a bell-shaped distribution along the frequency range. The percentage is in the range of 5 to 12% and the maximum absorption is observed almost at 10.5 GHz for all samples. This might be due to the minimum peak of the S_{11} for all samples are approximately at that frequency and furthermore the calculation only involves magnitude of S-parameters. However the absorption trend throughout the frequency range is possibly because of materials characteristic such as particle category and size, which later can be addressed as its specific resonant frequency. Absorption capability increases significantly when GO is introduced into polymer composite of $ZnFe_2O_4$ especially for 3 wt.% loading of GO. The GO itself shows the highest absorption among others because it has higher dielectric constant and loss as observed in Fig. 7(a).

Fig. 7(a) shows relative complex permittivity of all epoxy composite materials was calculated by NRW conversion technique based on measured S-parameters. The real part of permittivity, ε_r' for all epoxy composite materials are almost constant over measurement frequency range. This is due to the polarization that is almost independent of the frequency when electric field is applied, which contributes to the independent oscillation of the electric dipole moments with the microwave frequencies [49]. There are two types of polarization involved in this microwave study; space charge and dipolar. Space charge polarization (interfacial polarization) takes place in an interface of two different substituents of zinc ferrite compound that has different grain boundaries and interfaces. However, dipolar polarization arises from molecules with a permanent dipole moment that is able to change its orientation in an applied electric field. As the GO is carbonaceous material which possesses permanent dipoles, and thus the permittivity value attributed by the dipolar polarization. The GO has higher value of ε_r' than the $ZnFe_2O_4$ due to higher value of S_{11}. Greater value of the ε_r' is observed when the loading of GO in the epoxy $ZnFe_2O_4$ increases up to 3 wt. %. Additionally, there is also an increment in the dielectric loss that is due to an extra relaxation of electron during the polarization.

Similar behavior is found to the imaginary part of permittivity, which also increases in all samples throughout the frequency range. However, the GO and 3-GO-$ZnFe_2O_4$ values are almost overlapping with each other and slightly increasing to the maximum at about 10.5 GHz before gradually decreasing and remaining almost constant after 11.1 GHz. The overlapping phenomenon is because of similar weight percent (3 wt. %) content of GO inside the epoxy even though there is existence of $ZnFe_2O_4$ for another mixture, which shows less significant dielectric loss of $ZnFe_2O_4$ as compared to GO. Thus, the dielectric loss of 3-GO-$ZnFe_2O_4$ is dominantly contributed by the presence of GO. This can be deduced that both real and imaginary part of complex relative permittivity of the epoxy compos-

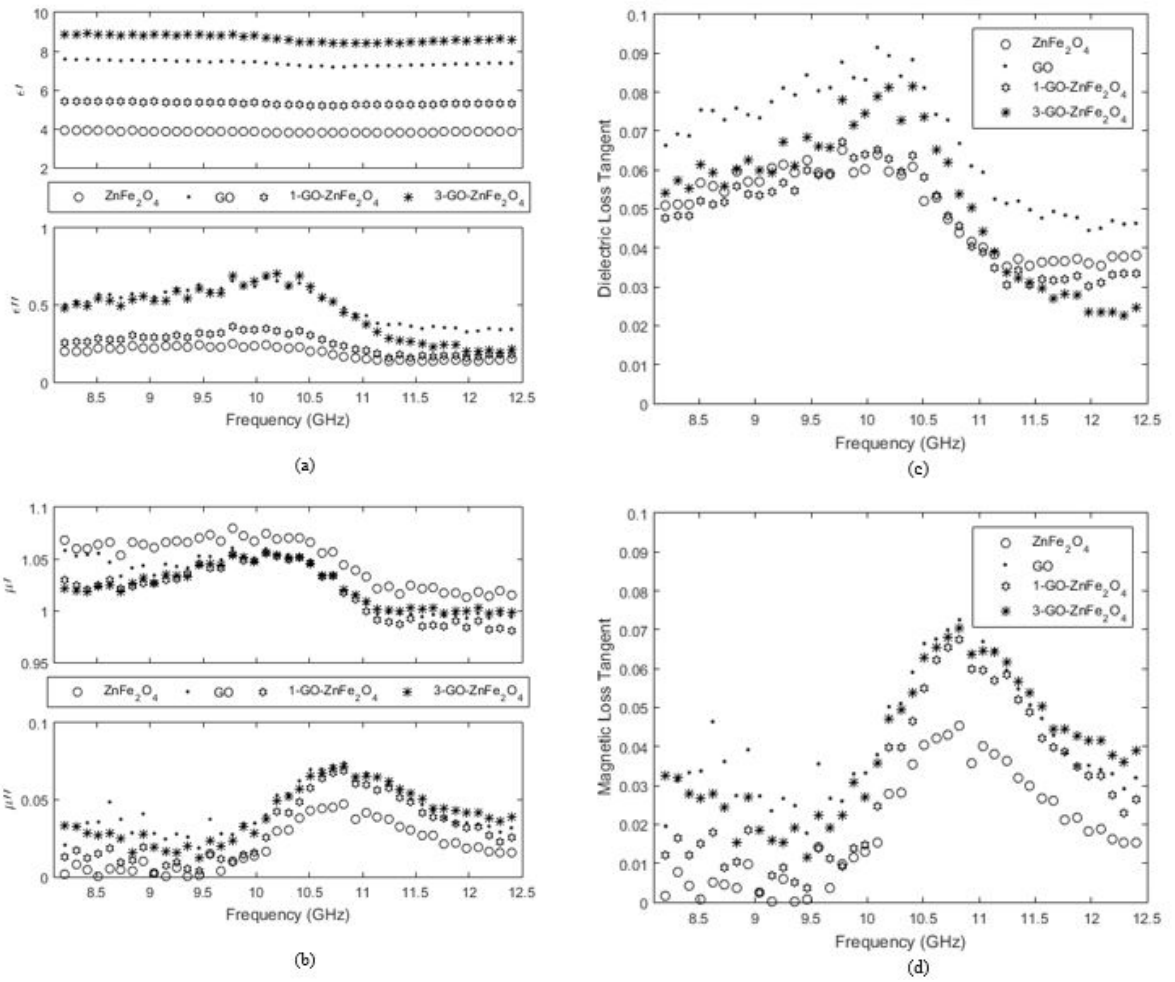

Fig. 7. Calculated value of (a) relative permittivity, (b) relative permeability, (c) dielectric and (d) magnetic loss tangent of epoxy composite materials.

ite materials can be changed with different amounts of GO fillers [49, 51, 52].

Fig. 7(b) shows the frequency dependence of the relative complex permeability for the samples. It can be seen that the real and imaginary part of permeability values lie in the ranges of 0.98 – 1.08 and 0 – 0.08, respectively. The real part of permeability of $ZnFe_2O_4$ is found to be slightly greater than the rest of composite materials along the frequency range because of magnetic behavior domination. Conversely, the magnetic loss has a low effect on electromagnetic wave attenuation hence small values of imaginary part of permeability are observed. In general, prediction of the magnetic loss for magnetic materials can be made based on magnetic hysteresis, eddy current, domain wall resonance, neutral resonance and exchange resonance. The eddy current loss can be associated with the electrical conductivity and thickness of the samples, and can be expressed by X_{eddy} [47].

$$X_{eddy} = \frac{\mu''}{f(\mu')^2} = 2\pi\mu_0\sigma d^2 \tag{10}$$

Similarly, the dielectric mechanism, μ_r' and μ_r'' also experienced the same behavior because of the increment in loss factor especially between range of 10 – 10.8 GHz where the μ_r' drops slightly in value. In general, the addition of GO filler in the epoxy composite of $ZnFe_2O_4$ is found to be having a minor change in complex relative permeability and this is also reported by some literatures [49, 51, 52]. The microwave absorption characteristics of the materials can be affected by small differences of the permeability [23]. Therefore, that is the reason of having an increment in the absorption percentage when GO content in polymer composite of $ZnFe_2O_4$ increases. Nevertheless, the absorption is essentially due to dielectric and magnetic dissipation factors from the intrinsic polymer composite material prop-

erties as shown in Fig. 7(c) and (d).

RL characteristic curve calculation was done using Equation 6 where effective input impedance (Equation 7) as the important parameter that requires EM properties retrieved from NRW earlier in this study. It is noticed that the concavities in the values of RL against frequency, suggesting a low reflectivity. Fig. 8 demonstrates the RL characteristic of $ZnFe_2O_4$, GO, 1-GO-$ZnFe_2O_4$ and 3-GO-$ZnFe_2O_4$ with the respective sample thicknesses as stated in Table 2. It is commonly known that the material with RL value less than -10 dB could be a potential candidate in microwave absorbing material application. This is due to approximation of 70% wave absorption upon reaching sample surface. Hence, there is a significant change on RL characteristic as the addition of GO filler increases especially for the 3-GO-$ZnFe_2O_4$, which is -12.5 dB at 10.5 GHz with thickness of 2.35 mm due to higher loss. The corresponding bandwidth related to the RL is 0.8 GHz, which is measured from 10.2 to 11 GHz. This proves that the dielectric material (GO) and the magnetic material ($ZnFe_2O_4$) can contribute equally to improve microwave absorption characteristics.

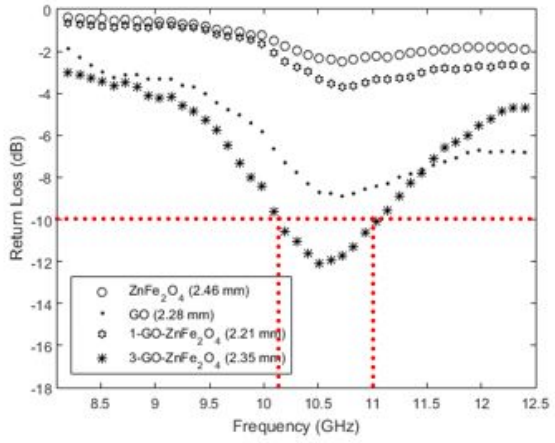

Fig. 8. RL characteristic of epoxy composite materials with different thicknesses.

According to the Equation 6, the RL characteristic of a composite material can be tuned and improved by changing the thickness of sample while maintaining the intrinsic electromagnetic properties of the composite material. For that reason, Fig. 9 presents the variation of calculated RL for each epoxy composite materials, $ZnFe_2O_4$, GO, 1-GO-$ZnFe_2O_4$ and 3-GO-$ZnFe_2O_4$ respectively at various thicknesses. The selected thicknesses are the optimum thicknesses where the return loss of each composite has been revealed at its minimum level. It is noticed that all occurs at about similar frequency, 10.5 GHz, which is very much related to the dissipation factor caused by dielectric and magnetic loss as mentioned earlier (Fig. 7). It can be seen that the 3-GO-$ZnFe_2O_4$ composite material performs as good as GO composite where the minimum RL is about -55 dB with reduction in thickness as much as 0.6 mm. The thickness was reduced from 7.8 mm to 7.2 mm, which signifies that a combination of dielectric filler and magnetic filler in polymer matrix host could have a lighter absorbing material without compromising the RL performance. The RL for $ZnFe_2O_4$ is only -18 dB with volumetric material 10.9 mm thick but when there is 1 wt.% additional of GO in 40 wt.% of total filler content, good enhancement of RL performance to -24 dB with 9.4 mm is observed. It is believed that by increasing GO content inside the polymer composite, a very significant performance of RL with lower thickness of sample will be attained. The sample can be used as a microwave absorbing coated material especially in the X-band frequency region. The summary of finding in Fig. 8 and 9 are presented in Table 4. Therefore, it can be noticed that each of composite samples with GO and $ZnFe_2O_4$ filler content reached minimum return loss due to the synergistic effect of both dielectric and magnetic loss and better impedance matching from the sample thickness with optimal addition of filler content [22, 51–53].

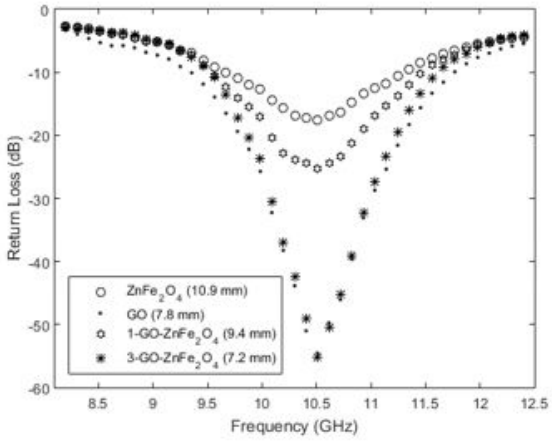

Fig. 9. RL characteristic of $ZnFe_2O_4$, GO, 1-GO-$ZnFe_2O_4$ and 3-GO-$ZnFe_2O_4$ at various thicknesses.

5. Conclusion

In conclusion, epoxy composite GO-$ZnFe_2O_4$ samples were successfully prepared by mixing GO and $ZnFe_2O_4$ in the epoxy matrix. The addition of GO filler content greatly affected the electromagnetic properties and return loss of GO-$ZnFe_2O_4$ composites due to the dielectric loss increment. The epoxy composite of 3-GO-$ZnFe_2O_4$ shows mini-

Table 4. Return loss of composite materials.

Composite materials	Sample thickness (mm)	Resonance frequency (GHz)	Minimum RL (dB)	Absorption (> 70%)	
				Range (GHz)	Bandwidth (GHz)
$ZnFe_2O_4$	2.46	10.8	-2.5	NA	NA
	10.90	10.5	-16.0	9.6 to 11.3	1.7
GO	2.28	10.6	-8.5	NA	NA
	7.80	10.5	-55.0	9.4 to 11.7	2.3
1-GO-	2.21	10.7	-3.8	NA	NA
$ZnFe_2O_4$	9.40	10.5	-25.0	9.5 to 11.4	1.9
3-GO-	2.35	10.5	-12.5	10.2 to 11	0.8
$ZnFe_2O_4$	7.20	10.5	-55.0	9.5 to 11.6	2.1

mum RL -12.7 dB at 10.5 GHz with 2.35 mm thickness and bandwidth 0.8 GHZ (from 10.2 to 11 GHz). Optimum performance of RL was successfully investigated by tuning the composite's thickness for each filler content. A minimum RL (-55 dB) is noticed for both GO and 3-GO-$ZnFe_2O_4$ with 7.8 mm and 7.2 mm thickness, respectively, suggesting that a lighter and thinner composite could be made while not compromising its performance. Further investigation into this study is highly recommended in future by selecting appropriate composition that can offer better RL characteristics at a minimum thickness of material, for example transparent absorber.

Acknowledgement

This study is supported by an internal grant TIER 1 from Universiti Tun Hussein Onn Malaysia under project number H233. A special thanks to Crest Nanosolutions (M) Sdn Bhd for the workshop on EM-30AX Plus Benchtop SEM (COXEM) that held in material physics laboratory, UTHM Pagoh Campus.

References

[1] Genban Sun, Bingxiang Dong, Minhua Cao, Bingqing Wei, and Changwen Hu. Hierarchical dendrite-like magnetic materials of Fe3O 4, γ-Fe2O3, and Fe with high performance of microwave absorption. *Chemistry of Materials*, 23(6):1587–1593, mar 2011.

[2] Fadzidah Mohd Idris, Mansor Hashim, Zulkifly Abbas, Ismayadi Ismail, Rodziah Nazlan, and Idza Riati Ibrahim. Recent developments of smart electromagnetic absorbers based polymer-composites at gigahertz frequencies. *Journal of Magnetism and Magnetic Materials*, 405:197–208, 2016.

[3] Tao Wang, Rui Han, Guoguo Tan, Jianqiang Wei, Liang Qiao, and Fashen Li. Reflection loss mechanism of single layer absorber for flake-shaped carbonyl-iron particle composite. *Journal of Applied Physics*, 112(10), nov 2012.

[4] Chun Ling Zhu, Mi Lin Zhang, Ying Jie Qiao, Gang Xiao, Fan Zhang, and Yu Jin Chen. Fe3O4/TiO2 core/shell nanotubes: Synthesis and magnetic and electromagnetic wave absorption characteristics. *Journal of Physical Chemistry C*, 114(39):16229–16235, oct 2010.

[5] H Gargama, A. K. Thakur, and S. K. Chaturvedi. Polyvinylidene fluoride/nanocrystalline iron composite materials for EMI shielding and absorption applications. *Journal of Alloys and Compounds*, 654:209–215, 2016.

[6] Zhou Wang and Guang-Lin Zhao. Microwave Absorption Properties of Carbon Nanotubes-Epoxy Composites in a Frequency Range of 2 - 20 GHz. *Open Journal of Composite Materials*, 03(02):17–23, 2013.

[7] F Qin and C Brosseau. A review and analysis of microwave absorption in polymer composites filled with carbonaceous particles, mar 2012.

[8] X. F. Zhang, X. L. Dong, H. Huang, Y. Y. Liu, W. N. Wang, X. G. Zhu, B. Lv, J. P. Lei, and C. G. Lee. Microwave absorption properties of the carbon-coated nickel nanocapsules. *Applied Physics Letters*, 89(5), 2006.

[9] Dongmao Jiao, Xiaodong Fan, Na Tian, Caiyin You, and Guojun Zhang. Improved magnetic and microwave absorption properties of manganese nitrides through the addition of ferrous. *Journal of Alloys and Compounds*, 703:13–18, 2017.

[10] Yu Chen, Hao Bin Zhang, Yaqin Huang, Yue Jiang, Wen Ge Zheng, and Zhong Zhen Yu. Magnetic and electrically conductive epoxy/graphene/carbonyl iron nanocomposites for efficient electromagnetic interference shielding. *Composites Science and Technology*, 118:178–185, 2015.

[11] Xiangqian Shen, Fuzhan Song, Xinchun Yang, Zhou Wang, Maoxiang Jing, and Yingde Wang. Hexaferrite/α-iron composite nanowires: Microstructure, exchange-coupling interaction and microwave absorption. *Journal of Alloys and Compounds*, 621:146–153, 2015.

[12] C. Hu, Z. Mou, G. Lu, N. Chen, Z. Dong, M. Hu, and

L. Qu. 3D graphene–Fe3O4 nanocomposites with high-performance microwave absorption. *Physical Chemistry Chemical Physics*, 15(31):13038–13043, 2013.

[13] Xin Sun, Jianping He, Guoxian Li, Jing Tang, Tao Wang, Yunxia Guo, and Hairong Xue. Laminated magnetic graphene with enhanced electromagnetic wave absorption properties. *Journal of Materials Chemistry C*, 1(4):765–777, 2013.

[14] Sachin Tyagi, Himanshu B. Baskey, Ramesh Chandra Agarwala, Vijaya Agarwala, and Trilok Chand Shami. Synthesis and characterization of microwave absorbing SrFe 12O 19/ZnFe 2O 4 nanocomposite. *Transactions of the Indian Institute of Metals*, 64(6):607–614, dec 2011.

[15] A Sutka, M Stingaciu, D Jakovlevs, and G. Mezinskis. Comparison of different methods to produce dense zinc ferrite ceramics with high electrical resistance. *Ceramics International*, 40(1 PART B):2519–2522, 2014.

[16] J P Singh, R S Payal, R C Srivastava, H M Agrawal, Prem Chand, Amita Tripathi, and R P Tripathi. Effect of thermal treatment on the magnetic properties of nanostructured zinc ferrite. In *Journal of Physics: Conference Series*, volume 217, page 12108, 2010.

[17] B Jeyadevan, K Tohji, and K Nakatsuka. Structure analysis of coprecipitated ZnFe2O4 by extended x-ray-absorption fine structure. *Journal of Applied Physics*, 76(10):6325–6327, 1994.

[18] M. K. Roy and H. C. Verma. Magnetization anomalies of nanosize zinc ferrite particles prepared using electrodeposition. *Journal of Magnetism and Magnetic Materials*, 306(1):98–102, 2006.

[19] G. F. Goya and H. R. Rechenberg. Ionic disorder and Néel temperature in ZnFe2O4 nanoparticles. *Journal of Magnetism and Magnetic Materials*, 196-197:191–192, 1999.

[20] C N Chinnasamy, A Narayanasamy, N Ponpandian, K Chattopadhyay, H Guérault, and J. M. Greneche. Magnetic properties of nanostructured ferrimagnetic zinc ferrite. *Journal of Physics Condensed Matter*, 12(35):7795–7805, 2000.

[21] Charles D.E. Lakeman and David A. Payne. Sol-gel processing of electrical and magnetic ceramics, 1994.

[22] Xiaodi Weng, Bingzhen Li, Yang Zhang, Xuliang Lv, and Guangxin Gu. Synthesis of flake shaped carbonyl iron/reduced graphene oxide/polyvinyl pyrrolidone ternary nanocomposites and their microwave absorbing properties. *Journal of Alloys and Compounds*, 695:508–519, 2017.

[23] Fen Li, Xue Jiang, Jijun Zhao, and Shengbai Zhang. Graphene oxide: A promising nanomaterial for energy and environmental applications, 2015.

[24] Tapas Kuila, Saswata Bose, Ananta Kumar Mishra, Partha Khanra, Nam Hoon Kim, and Joong Hee Lee. Chemical functionalization of graphene and its applications, 2012.

[25] Han Hu, Zongbin Zhao, Quan Zhou, Yury Gogotsi, and Jieshan Qiu. The role of microwave absorption on formation of graphene from graphite oxide. *Carbon*, 50(9):3267–3273, 2012.

[26] Yiqing Sun, Qiong Wu, and Gaoquan Shi. Graphene based new energy materials, 2011.

[27] Yunchen Du, Wenwen Liu, Rong Qiang, Ying Wang, Xijiang Han, Jun Ma, and Ping Xu. Shell thickness-dependent microwave absorption of core-shell Fe 3O4@C composites. *ACS Applied Materials and Interfaces*, 6(15):12997–13006, aug 2014.

[28] Hui Zhang, Anjian Xie, Cuiping Wang, Haisheng Wang, Yuhua Shen, and Xingyou Tian. Novel rGO/α-Fe2O3 composite hydrogel: Synthesis, characterization and high performance of electromagnetic wave absorption. *Journal of Materials Chemistry A*, 1(30):8547–8552, 2013.

[29] Rajesh Kumar, Rajesh Kumar Singh, Jai Singh, R. S. Tiwari, and O. N. Srivastava. Synthesis, characterization and optical properties of graphene sheets-ZnO multipod nanocomposites. *Journal of Alloys and Compounds*, 526:129–134, 2012.

[30] N. Campo and A. M. Visco. Incorporation of carbon nanotubes into ultra high molecular weight polyethylene by high energy ball milling. *International Journal of Polymer Analysis and Characterization*, 15(7):438–449, 2010.

[31] Hoda Hekmatara, Majid Seifi, Keyvan Forooraghi, and Sharareh Mirzaee. Synthesis and microwave absorption characterization of SiO2 coated Fe3O4-MWCNT composites. *Physical Chemistry Chemical Physics*, 16(43):24069–24075, 2014.

[32] Puleng N. Mbuyisa, Federica Rigoni, Luigi Sangaletti, Stefano Ponzoni, Stefania Pagliara, Andrea Goldoni, Muzi Ndwandwe, and Cinzia Cepek. Growth of hybrid carbon nanostructures on iron-decorated ZnO nanorods. *Nanotechnology*, 27(14), 2016.

[33] Yujin Chen, Zhenyu Lei, Hongyu Wu, Chunling Zhu, Peng Gao, Qiuyun Ouyang, Li Hong Qi, and Wei Qin. Electromagnetic absorption properties of graphene/Fe nanocomposites. *Materials Research Bulletin*, 48(9):3362–3366, 2013.

[34] Olli Luukkonen, Stanislav I. Maslovski, and Sergei A. Tretyakov. A stepwise Nicolson-Ross-Weir-based material parameter extraction method. *IEEE Antennas and Wireless Propagation Letters*, 10:1295–1298, 2011.

[35] Toru Maeda, Satoshi Sugimoto, Toshio Kagotani, Nobuki Tezuka, and Koichiro Inomata. Effect of the soft/hard exchange interaction on natural resonance frequency and electromagnetic wave absorption of the rare earth-iron-boron compounds. *Journal of Magnetism and Magnetic Materials*, 281(2-3):195–205, 2004.

[36] N.B. Singh and A. Agarwal. Preparation, characterization, properties and applications of nano zinc ferrite. *Materials Today: Proceedings*, 5(3):9148–9155, 2018.

[37] Pingxin Liu, Yueming Ren, Wenjie Ma, Jun Ma, and Yunchen Du. Degradation of shale gas produced water by magnetic porous MFe2O4 (M = Cu, Ni, Co and Zn) heterogeneous catalyzed ozone. *Chemical Engineering Journal*, 345:98–106, 2018.

[38] Ruiwen Shu, Gengyuan Zhang, Jiabin Zhang, Xin Wang, Meng Wang, Ying Gan, Jianjun Shi, and Jie He. Synthesis and high-performance microwave absorption of reduced graphene oxide/zinc ferrite hybrid nanocomposite. *Materials Letters*, 215:229–232, 2018.

[39] Oguz Bayindir and Murat Alanyalioglu. Azure B Nanocomposites of Chemically and Electrochemically Produced Graphene Oxide: Comparison of Amperometric Sensor Performance for NADH. *IEEE Sensors Journal*, 19(3):812–819, 2019.

[40] K. Kishore Kumar, R. Brindha, M. Nandhini, M. Selvam, K. Saminathan, and K. Sakthipandi. Water-suspended graphene as electrolyte additive in zinc-air alkaline battery system. *Ionics*, 25(4):1699–1706, apr 2019.

[41] Sedigheh Dadras and Maryam Faraji. Improved carbon nanotube growth inside an anodic aluminum oxide template using microwave radiation. *Journal of Physics and Chemistry of Solids*, 116:203–208, 2018.

[42] M. Selvam, K. Sakthipandi, R. Suriyaprabha, K. Saminathan, and V. Rajendran. Synthesis and characterization of electrochemically-reduced graphene. *Bulletin of Materials Science*, 36(7):1315–1321, 2013.

[43] Karthikeyan Krishnamoorthy, Murugan Veerapandian, Kyusik Yun, and S. J. Kim. The chemical and structural analysis of graphene oxide with different degrees of oxidation. *Carbon*, 53:38–49, 2013.

[44] Harish Mudila, Sweta Rana, and M. G.H. Zaidi. Electrochemical performance of zirconia/graphene oxide nanocomposites cathode designed for high power density supercapacitor. *Journal of Analytical Science and Technology*, 7(1), dec 2016.

[45] Geetika Khurana, Nitu Kumar, Sudheendran Kooriyattil, and Ram S. Katiyar. Structural, magnetic, and dielectric properties of graphene oxide/ZnxFe1-xFe2O4 composites. *Journal of Applied Physics*, 117(17), may 2015.

[46] Xin Geng, Da Wei He, Yong Sheng Wang, Wen Zhao, Yi Kang Zhou, and Shu Lei Li. Synthesis and microwave absorption properties of graphene-oxide(GO)/polyaniline nanocomposite with Fe3O4 particles. *Chinese Physics B*, 24(2), 2015.

[47] Ruiwen Shu, Gengyuan Zhang, Jiabin Zhang, Xin Wang, Meng Wang, Ying Gan, Jianjun Shi, and Jie He. Fabrication of reduced graphene oxide/multi-walled carbon nanotubes/zinc ferrite hybrid composites as high-performance microwave absorbers. *Journal of Alloys and Compounds*, 736:1–11, 2018.

[48] CC Chen, WF Liang, YH Nien, HK Liu Materials Research Bulletin, and Undefined 2017. Microwave absorbing properties of flake-shaped carbonyl iron/reduced graphene oxide/epoxy composites. *Materials Research Bulletin*, 96:81–85, 2017.

[49] Lingyu Zhu, Xiaojun Zeng, Xiaopan Li, B Yang, and Ronghai Yu. Hydrothermal synthesis of magnetic Fe3O4/graphene composites with good electromagnetic microwave absorbing performances. *Journal of Magnetism and Magnetic Materials*, 426:114–120, 2017.

[50] Asish Malas, Avanish Bharati, Olivier Verkinderen, Bart Goderis, Paula Moldenaers, and Ruth Cardinaels. Effect of the GO reduction method on the dielectric properties, electrical conductivity and crystalline behavior of PEO/rGO nanocomposites. *Polymers*, 9(11), 2017.

[51] Sanghamitra Acharya, J Ray, T. U. Patro, Prashant Alegaonkar, and Suwarna Datar. Microwave absorption properties of reduced graphene oxide strontium hexaferrite/poly(methyl methacrylate) composites. *Nanotechnology*, 29(11), 2018.

[52] Dezhi Chen, Guang Sheng Wang, Shuai He, Jia Liu, Lin Guo, and Mao Sheng Cao. Controllable fabrication of mono-dispersed RGO-hematite nanocomposites and their enhanced wave absorption properties. *Journal of Materials Chemistry A*, 1(19):5996–6003, 2013.

[53] Vivek K. Singh, Anuj Shukla, Manoj K. Patra, Lokesh Saini, Raj K. Jani, Sampat R. Vadera, and Narendra Kumar. Microwave absorbing properties of a thermally reduced graphene oxide/nitrile butadiene rubber composite. *Carbon*, 50(6):2202–2208, 2012.